Archives of Microbiology (2024) 206:324
https://doi.org/10.1007/s00203-024-04059-4

BRIEF REPORT

Citral and triclosan synergistically silence quorum sensing and potentiate antivirulence response in Pseudomonas aeruginosa

Jatin Chadha[1] · Prerna Ahuja[1] · Umang Mudgil[1] · Lavanya Khullar[1] · Kusum Harjai[1]

Received: 18 May 2024 / Revised: 6 June 2024 / Accepted: 17 June 2024 / Published online: 24 June 2024

Abstract

Among the ESKAPE pathogens, *Pseudomonas aeruginosa* is an extensively notorious superbug that causes difficult-to-treat infections. Since quorum sensing (QS) directly promotes pseudomonal virulence, targeting QS circuits is a promising approach for disarming phenotypic virulence. Hence, this study scrutinizes the anti-QS, antivirulence, and anti-biofilm potential of citral (CiT; phytochemical) and triclosan (TcN; disinfectant), alone and in combination, against *P. aeruginosa* PAO1/PA14. The findings confirmed synergism between CiT and TcN and revealed their quorum quenching (QQ) potential. At sub-inhibitory levels, CiT-TcN combination significantly impeded pyocyanin, total bacterial protease, hemolysin, and pyochelin production alongside inhibiting biofilm formation in *P. aeruginosa*. Moreover, the QQ and antivirulence potential of CiT and TcN was positively correlated by molecular docking studies that predicted strong associations of the drugs with QS receptors of *P. aeruginosa*. Collectively, the study identifies CiT-TcN as an effective drug combination that harbors QQ, antivirulence, and anti-biofilm prospects against *P. aeruginosa*.

Communicated by Yusuf Akhter.

Jatin Chadha and Prerna Ahuja contributed equally to this work.

✉ Kusum Harjai
kusumharjai@pu.ac.in

[1] Department of Microbiology, Panjab University, Chandigarh, India

Graphical abstract

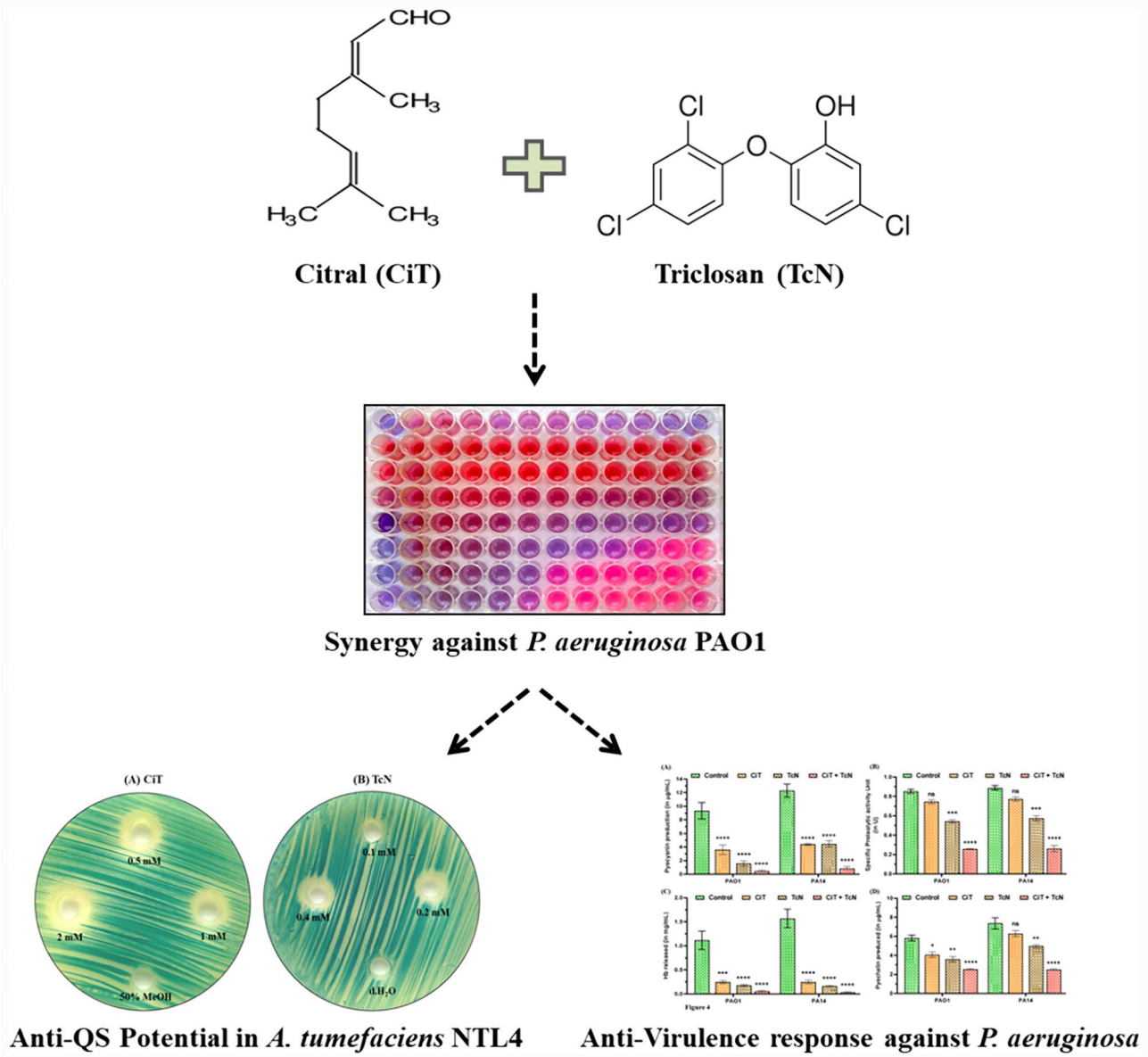

Keywords Citral · Triclosan · Pseudomonas aeruginosa · Quorum quenching · Virulence · Biofilm inhibition

Abbreviations

AHL	Acyl-homoserine lactone
CiT	Citral
CV	Crystal violet
MIC	Minimum inhibitory concentration
QQ	Quorum quenching
QS	Quorum sensing
TcN	Triclosan

Introduction

The overexploitation and unregulated consumption of antimicrobial agents has resulted in the emergence of drug-resistant microorganisms (Chadha and Khullar 2021), thereby lowering the effectiveness of conventional antibiotics in mitigating common bacterial diseases and accelerating the silent antimicrobial resistance (AMR) pandemic (Laxminarayan 2022). Among the ESKAPE pathogens, *Pseudomonas aeruginosa* (Carbepenam-resistant), recently

categorized as a high priority superbug by the World Health Organization (WHO), is one of the most notorious and extensively drug-resistant Gram-negative bacterium (WHO 2024). Owing to the production of diverse virulence factors, resilient biofilms, and numerous intrinsic/extrinsic mechanisms of drug resistance, *P. aeruginosa* causes hard-to-treat infections (Chadha et al. 2021b). Moreover, the pathogen exhibits wide tissue tropism and causes a plethora of infections in immunocompromised individuals like catheter-associated urinary tract infections, cystic fibrosis, keratitis, respiratory tract-, burn wound-, and bone- and joint infections (Qin 2022). Hence, alternative strategies such as antivirulence therapy employing nutraceuticals can prove to be effective in managing pseudomonal infections (Chadha et al. 2021a). Interestingly, the virulence of *P. aeruginosa* is stringently modulated by a cell-density-dependent mechanism called quorum sensing (QS) (Moradali et al. 2017). The Las, Rhl, and Pqs signaling pathways work in a synchronous manner to regulate the social behavior of the pathogen, thereby inducing the expression of virulence genes and contributing to bacterial pathogenesis, adaptation/survival, and persistence (Chadha et al. 2021b). Therefore, abrogating the QS mechanisms (quorum quenching; QQ) in *P. aeruginosa* can effectively disarm bacterial virulence and reduce disease progression/severity. Additionally, QQ does not extend any selection pressure since bacterial killing is completely avoided/by-passed and only QS pathways that promote pseudomonal virulence are specifically silenced (Moradali et al. 2017; Chadha et al. 2021a).

In this context, the scientific community has been actively exploring naturally-occurring antivirulence agents such as plant extracts, essential oils (EOs), and their bioactive components (Chadha et al. 2021a). Due to their natural abundance, easy availability, cost-effectiveness, and multifaceted pharmacological properties, phytochemicals are drawing immense popularity in mainstream medicine (Chadha et al. 2021c). Among these, citral (CiT), the principle bioactive phytocompound of lemongrass oil (65–85%), is extensively used in perfumery, flavouring agent, and cosmetic products. It is known to possess various biological properties including antimicrobial, and antifouling activity against multiple bacterial pathogens (Manganelli et al. 2016; Kang et al. 2022; Dai et al. 2023). Recently, CiT and its nanoformulation were shown to be effective in disrupting QS and curtailing bacterial virulence in *P. aeruginosa* (Sharma et al. 2023). Furthermore, triclosan (TcN), a highly potent antimicrobial halogenated aromatic hydrocarbon, has been widely explored for its quorum quenching activity against *Chromobacterium violaceum* LMG 1267 (Fidaleo et al. 2013) and *Vibrio harveyi* BB170 (Kaur et al. 2022) by targeting the acyl-homoserine lactone (AHL)- and autoinducer-2-dependent QS mechanisms, respectively. TcN has also found application in a wide range of personal care products such as disinfectants, hand sanitizers, detergents, soaps, and hand/mouth washes (Sinicropi et al. 2022). Considering the widespread use of these agents commercially, this study was undertaken to scrutinize the antibacterial, anti-QS, and anti-biofilm potential of CiT-TcN combination. Drug interactions were studied for exploring the antivirulence potential of this combination against *P. aeruginosa* PAO1 and PA14 using in vitro experimentation and in silico analysis.

Materials and methods

Bacterial cultures, growth media, and chemicals

Standard strains, *P. aeruginosa* PAO1 (ATCC 15692), *P. aeruginosa* PA14 (ATCC 15442), and *Agrobacterium tumefaciens* NTL4 (pZLR4), were procured from Dr. Barbara H. Iglweski, University of Rochester (NY, USA), Dr. Jogender Singh, IISER Mohali (India), and Dr. Jo Handelsman, Wisconsin University (WI, USA), respectively. Cultures were raised in nutrient broth (NB) (HiMedia Labs, Mumbai, India) containing gentamicin (50 µg/mL) at 37 ℃ and 30 ℃, respectively. Citral (CiT) and Triclosan (TcN) were purchased from Sigma-Aldrich (MO, USA) and their stock solutions were prepared in 50% methanol (MeOH) and sterile distilled water, respectively.

Determination of minimum inhibitory concentration (MIC) and sub-MIC against P. aeruginosa

The MIC of CiT and TcN was determined against *P. aeruginosa* PAO1 and PA14 using the standard microbroth dilution method (Wiegand et al. 2008). Briefly, two-fold serial dilutions of the test agents were prepared individually in 96-well microtiter plates containing double-strength MH broth and inoculated with bacterial cultures harboring 1×10^8 CFU/mL. Sterile MH broth served as negative control while inoculated MH broth (lacking drugs) served as positive control. Ciprofloxacin was also used as the antibiotic control (standard) for the experiment. Post overnight incubation at 37 ℃, 20 µL of resazurin dye (0.01%) was added to every well and further incubated for 2 h. The lowest drug concentration that prevented resazurin reduction (from dark blue to pink) was reported as the MIC. Subsequently, the drug concentrations that fail to inhibit bacterial growth, termed sub-MICs, were determined by monitoring the growth pattern of pseudomonal cultures in the presence and absence of test drugs (Chadha et al. 2021a). For this, overnight cultures of PAO1 and PA14 were inoculated (1%) in NB flasks containing 1/2, 1/4, 1/8, and 1/16 MIC of CiT and TcN (independently) and incubated at 37 ℃ with shaking at 160 rpm. Over a 24 h period with 2 h interval,

the growth profile was monitored spectrophotometrically at 600 nm. Drug concentrations that extended minimal or no effect on bacterial growth were selected as the sub-MICs for further experimentation.

Checkerboard assay for determining drug interactions

To examine the type of interaction between CiT and TcN, a standardized checkerboard assay was employed (Chadha et al. 2022). In a 96 well microtiter plate containing double-strength MH broth, two-fold serial dilutions of CiT and TcN, alone and in combination, were prepared in vertical and horizontal orientations, respectively. PAO1 and PA14 cultures harboring 1×10^8 CFU/mL were added to each well (separate plates) and incubated overnight at 37 ℃. Wells containing sterile MH broth served as negative control while those containing inoculated broth (lacking drugs) were used as positive growth control. Post-incubation, bacterial growth/inhibition was assessed using the resazurin-based dye-reduction method. The fractional inhibitory concentration (FIC) index was then calculated to assess the drug interaction using the following formula: FIC of drug = MIC in combination/MIC alone, FIC index = FIC of CiT + FIC of TcN. The FIC index (FICI) was interpreted as follows: FICI ≤ 0.5 (synergy), 0.5 ≤ FIC ≤ 1.0 (additive), 1.0 ≤ FIC ≤ 2.0 (indifferent), and FICI ≥ 4.0 (antagonism) (Chadha et al. 2022).

Qualitative assay for anti-QS potential

The QS biosensor strain, *A. tumefaciens* NTL4, was employed to qualitatively examine the quorum quenching potential of CiT and TcN (Chadha et al. 2023a). Initially, acyl-homoserine lactones (AHLs) were isolated from an overnight-grown culture of *P. aeruginosa* PAO1 using the solvent-based extraction method (Harjai et al. 2016). Next, the biosensor assay was performed by sequentially spread plating 150 µL of X-Gal (8 mg/mL) and extracted AHLs, followed by evenly swabbing 200 µL of *A. tumefaciens* NTL4 culture (A_{600} ~ 0.8) onto an MHA plate. After air drying, wells were punched using a sterile borer and 100 µL of CiT (0.5, 1, 2 mM) and TcN (0.1, 0.2, 0.4 mM) were dispensed in separate wells. Respective solvents served as control for the experiment. Post 48 h incubation at 30 ℃, zones of colourless halo around the wells were recorded to assess the anti-QS potential.

Effect on production of QS-regulated virulence factors

The phenotypic expression of hallmark QS-regulated virulence factors of *P. aeruginosa* PAO1 and PA14 was scrutinized following treatment with sub-MICs of CiT (3.92 mM) and TcN (0.12 mM), alone and in combination. Briefly, overnight-grown cultures of *P. aeruginosa* (drug-treated and -untreated) were diluted using sterile broth to normalize cell density across various experimental groups (A_{600} ~ 0.8), followed by centrifugation at $10{,}000 \times g$ for 10 min. The cell-free supernatants were collected separately and then used for further experimentation involving quantitative estimation of pyocyanin, pyochelin, total protease, and hemolysin production using previously-established laboratory methods (Chadha et al. 2022, 2023b). The percentage reduction/fold change was calculated by normalizing the data with control group (untreated PAO1/PA14).

Effect on pseudomonal biofilm formation

Qualitative crystal violet (CV)-binding assay was performed to evaluate the anti-biofilm potential of CiT (3.92 mM) and TcN (0.12 mM) against *P. aeruginosa* PAO1 and PA14 (Bose et al. 2020). Concisely, NB tubes (glass) supplemented with CiT (mM) and TcN (mM) at sub-inhibitory concentrations, alone and in combination, were independently inoculated with cultures of PAO1/PA14 (1 X 10^8 CFU/mL) and incubated under static conditions for 72 h to permit biofilm formation. Post-incubation, the spent media was discarded and the glass tubes were washed thrice with sterile PBS (pH 7.2) to remove any planktonic cells. Next, the adherent biofilms were stained using 0.1% CV for 20 min at room temperature, followed by three rounds of gentle washing to remove unbound stain. Based on the intensity of bound CV, adherence scores were assigned to each experimental group (control, CiT and TcN: alone and in combination) which were ultimately used for qualitatively assessing the biofilm-forming ability of *P. aeruginosa*. Biofilm-forming capacity was denoted in terms of adherence scores: (+++) strong biofilm, (++) moderate biofilm, (+) weak biofilm, and (−) no biofilm. Further, biofilm inhibition was quantified by eluting the adherent CV using 1 mL of 33% glacial acetic acid and recording the A_{595} values (Chadha 2021).

Ligand standardization and molecular docking

Molecular docking was undertaken to compute the possible atomic interactions with CiT and TcN with the QS receptors of *P. aeruginosa* (Bose et al. 2020). The structures of LasR (PDB: 3IX3), PqsR (PDB: 4JVC), and RhlR (PDB: 8B4A) were retrieved from Protein Data Bank (PDB) (https://www.rcsb.org/), followed by removal of water molecules and native ligands. Energy minimization was carried out using GROMACS software suite (v2020.6) employing CharMM36 force field, followed by the addition of polar hydrogens and Kollman charges using AutoDock Tools. The docking grid

was generated based on the molecular interactions defined between the QS receptor and its native ligand (see Table 1). The structures of CiT (PubChem CID: 638,011) and TcN (PubChem CID: 5564), 3-oxo-C12-HSL (PubChem CID: 3,246,941), C4-HSL (PubChem CID: 443,433), and PQS (PubChem CID: 2,763,159) were retrieved from PubChem (sdf format) and converted to 3D structures (with polar hydrogens) using Open Babel. The exhaustiveness was set to '24' and docking was then performed using AutoDock Vina (Version 1.5.4). The best binding pose (out of 9 poses obtained) was selected based on the predicted binding energy (kcal/mol) and molecular interactions between the receptor-ligand complexes. Native ligands were also docked to validate the computational findings. Comparisons were then drawn between the docking scores (binding energies) obtained with CiT/TcN and the native ligand of each QS receptor.

Statistical analysis

Every experiment was performed thrice independently in a set of three biological replicates. The results/experimental values have been represented as mean ± standard deviation. All graphs were generated using GraphPad Prism (ver. 8.0) and the significance of data was analyzed using one-way analysis of variance (ANOVA) test. Tukey's multiple comparisons test was also used to examine datasets across multiple experimental groups. p-values of < 0.05 were regarded as statistically significant (p-values: * ≤ 0.05, ** ≤ 0.01, *** ≤ 0.001, **** ≤ 0.0001).

Results and discussion

CiT and TcN alter the growth profile of *P. aeruginosa*

The microbroth dilution method coupled with resazurin dye reduction test was employed to determine the MICs of CiT and TcN against *P. aeruginosa*. With CiT, the MIC was experimentally found to be 32.5 mM, while TcN yielded MIC value of 6.88 mM against both PAO1 and PA14 (Figure S1). Since the primary objective of the study was to investigate the QQ potential of CiT and TcN at sub-lethal concentrations, we further examined the growth profile of *P. aeruginosa* in the presence and absence of test agents at different sub-MICs. Untreated (control) groups of PAO1 and PA14 revealed characteristic sigmoidal curves indicating ideal bacterial growth with distinct lag, log, and stationary phases (Fig. 1). Interestingly, both CiT and TcN inhibited bacterial growth in a concentration-dependent manner with

Table 1 Binding energies and predicted molecular interactions between CiT/TcN and QS receptors of *P. aeruginosa* using AutoDock Vina (version 1.5.4)

QS receptors	Ligands	Binding energy (kcal/mol)	Interacting amino acid residues
LasR	3-oxo-12-HSL	− 8.2	Leu36, Gly38, Tyr47, Ile52, Tyr56, Trp60, Arg61, Tyr64, Ala70, Asp73, Thr75, Val76, Trp88, Tyr93, Phe101, Ala105, Leu110, Thr115, Gly126, Ala127, Ser129
	CiT	− 6.8	**Leu36**, **Ile52**, **Tyr56**, **Trp60**, **Arg61**, **Tyr64**, **Asp73**, **Thr75**, **Val76**, **Trp88**, **Tyr93,** Phe101, **Ala105**, **Leu110**, **Ser129**
	TcN	− 9.0	**Leu36**, **Ile52**, **Tyr56**, **Trp60**, **Arg61**, **Tyr64**, **Ala70**, **Asp73**, **Thr75**, **Val76**,**Trp88**, **Tyr93**, **Phe101**, **Ala105**, **Leu110**, **Thr115**, **Ala127**, **Ser129**
	Furanone C-30	− 6.6	Leu36, Tyr47, Ala50, Ile52, Tyr56, Trp60, Arg61, Tyr64, Thr75, Val76, Ala127, Ser129
PqsR	PQS	− 7.0	Ile149, Ala168, Val170, Ser196, Leu197, Leu207, Leu208, Phe221, Met224, Ile236, Tyr258, Ile263, Thr265
	CiT	− 5.7	**Pro129**, **Ile149**, **Ala168**, **Gln194**, Ile195, **Ser196**, **Leu197**, **Leu208**, **Phe221**, **Met224**, **Gly235**, **Ile236**, **Ala237**, **Pro238**
	TcN	− 6.4	**Ile149**, **Val170**, **Leu197**, **Leu207**, **Leu208**, Val211, **Phe221**, **Ile236**, **Ile263**, **Thr265**
	Furanone C-30	− 5.7	Ala102, Ser128, Pro129, Ala130, Ile149, Gln194, Leu197, Leu208, Phe221, Ile236, Ala237, Pro238
RhlR	C4-HSL	− 6.6	Ala44, Val60, Tyr64, Trp68, Tyr72, Asp81, Ala83, Ile84, Trp96, Phe101, Leu107, Trp108, Ala111, Thr121, Ser135
	CiT	− 6.2	**Val60**, **Tyr64**, **Trp68**, **Tyr72**, **Asp81**, **Ala83**, **Ile84**, **Trp96**, **Phe101**, **Leu107**, **Trp108**, **Ala111**, **Thr121**, **Ser135**
	TcN	− 8.4	Gly46, **Val60**, **Tyr64**, **Trp68**, **Tyr72**, **Asp81**, **Ala83**, **Ile84**, **Trp96**, **Phe101**, **Leu107**, **Trp108**, **Ala111**, Leu116, **Thr121**, **Ser135**
	Furanone C-30	− 5.9	Ala44, Val60, Trp68, Tyr72, Asp81, Ala83, Trp96, Leu107, Val133, Ser135

Boldface amino acid residues interacting with CiT/TcN were found to have overlapping interactions with that of either the natural ligand of each QS receptor or furanone C-30

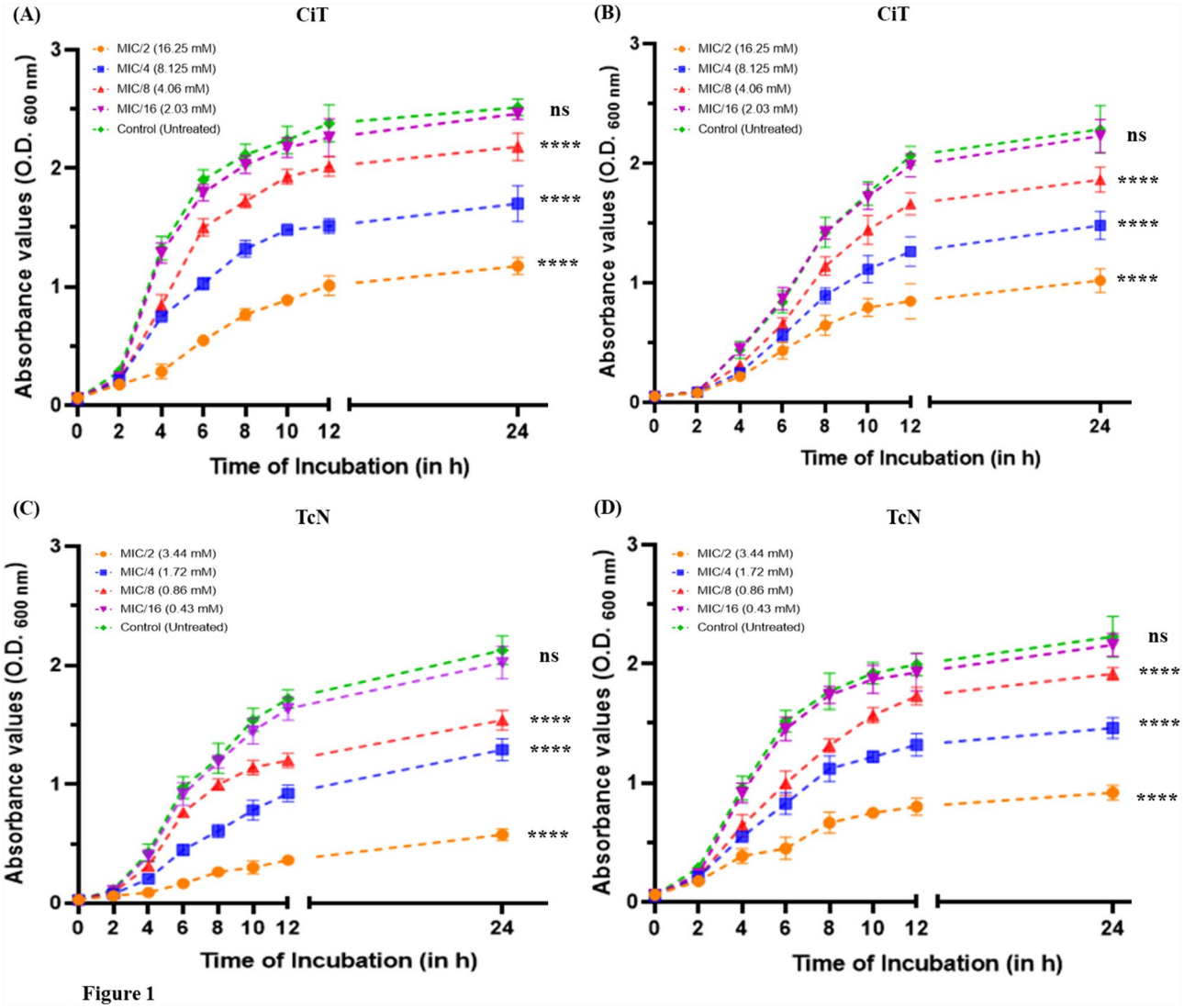

Fig. 1 Growth profile of *P. aeruginosa* PAO1 (**A**, **C**) and *P. aeruginosa* PA14 (**B**, **D**) in the presence and absence of CiT and TcN at various test sub-MICs. *ns* no significance, $p^{****} \leq 0.0001$

high drug levels abrogating pseudomonal growth during early time points. At sub-MICs of 1/2, 1/4, and 1/8, both CiT (Fig. 1A, B) and TcN (Fig. 1C, D) were able to effectively inhibit the growth of PAO1 and PA14 as evident by early saturation in absorbance values. Nevertheless, upon lowering the drug concentrations to 1/16 MIC of CiT and TcN, the inhibitory effect was subdued and the growth profiles of PAO1 and PA14 closely resembled their untreated (control) counterparts (Fig. 1). Since the drugs got diluted to empirically lower sub-lethal concentrations (Chadha and Khullar 2021), the growth inhibition was overcome and bacterial proliferation occurred steadily. Hence, for conducting antivirulence-related studies and overcoming bactericidal effects, CiT and TcN were used at concentrations below 2.03 mM and 0.43 mM, respectively.

CiT and TcN independently exhibit quorum quenching potential

In pursuit of investigating the antivirulence potential of CiT and TcN, we first examined their anti-QS potential using the *A. tumefaciens* NTL4, a genetically-modified biosensor strain that shows both short- and long-chain AHL-induced expression of β-galactosidase from pZLR4 (Chadha et al. 2023a). Under ideal conditions, AHLs induce QS through the *traI* promotor on pZLR4 which results in β-galactosidase-mediated degradation of X-gal, thereby yielding a blue-coloured bacterial lawn. However, upon effective QQ, production of β-galactosidase is abrogated which leads to development of off-white coloured bacterial growth (Chadha et al. 2022). Interestingly, both CiT and TcN

at sub-MIC levels resulted in notable anti-QS zones characterized by the loss of blue coloration (quenching) (Fig. 2). Wells loaded with 0.5, 1.0, and 2.0 mM of CiT revealed anti-QS zones (diameter) of 6.43 ± 0.453, 6.29 ± 0.364, and 8.51 ± 0.408 mm, respectively (Fig. 2A). Contrarily, TcN at concentrations of 0.2 and 0.4 mM yielded anti-QS zones of 5.57 ± 0.416 and 6.5 ± 0.462 mm, respectively (Fig. 2B). The results clearly indicated that CiT and TcN independently are capable of disrupting AHL-mediated pathways of QS. These findings are in sync with recent reports that highlight the role of CiT (Batohi et al. 2021; Sharma et al. 2023) and TcN (Fidaleo et al. 2013) in abrogating autoinducer-mediated QS in *C. violaceum* and *P. aeruginosa*. Therefore, these findings provide fertile grounds for exploring the antivirulence potential of CiT and TcN against *P. aeruginosa*.

Checkerboard assay reveals synergism between CiT and TcN against *P. aeruginosa*

Since both the test agents independently displayed QQ properties, we were intrigued to investigate their drug interactions against *P. aeruginosa*. This was undertaken using a previously-reported checkerboard assay coupled with resazurin dye reduction (Chadha et al. 2023b). When used in combination, the MIC values of CiT and TcN drastically reduced by ~ 8- and 28-folds against PAO1, respectively (Fig. 3A). Similarly, combining CiT and TcN together resulted in further lowering of individual MIC values by ~ 8- and 56-fold against *P. aeruginosa* PA14, respectively (Fig. 3B). The FIC index for CiT-TcN combination against PAO1 and PA14 was found to be 0.156 and 0.138, respectively, pointing towards a strong synergistic interaction between the two drugs. In this context, previous reports have unraveled the synergistic interaction of CiT/TcN with various antibiotics (Tabak et al. 2009; Shrestha et al. 2020) and phytochemicals (Cao et al. 2021; Valliammai et al. 2021) against bacterial pathogens. These findings underscore the potential for combining CiT and TcN to achieve enhanced antimicrobial efficacy against the pathogen. Therefore, the drug combination can be deemed highly effective against *P. aeruginosa*.

CiT-TcN combination phenotypically silences pseudomonal virulence

Considering the QQ potential and synergistic interaction displayed by CiT and TcN, we then assessed their role in potentiating antivirulence response against *P. aeruginosa*. For this, cultures of PAO1 and PA14 were raised in the presence and absence of CiT and TcN (at sub-synergistic concentrations), alone and in combination, and QS-regulated hallmark virulence factors, including pyocyanin, hemolysin, pyochelin, and protease production, were quantified in cell-free supernatants using standard assays (Chadha et al. 2022). Pyocyanin is a unique blue-coloured pseudomonal pigment that disturbs ciliary activity, triggers oxidative stress, and extends cytotoxicity by promoting the generation of reactive oxygen species (Chadha et al. 2021b). The secretion of hemolysins by *P. aeruginosa* facilitates erythrolysis (RBC degradation) via phospholipid hydrolysis, which thereby aids in sequestering iron from hemoglobin (iron acquisition) through chelation by bacterial siderophores (pyochelin/pyoverdine) (Chadha et al. 2021b). Hydrolytic enzymes such as LasA protease and LasB elastase promote degradation of immunomodulatory proteins and constituents of extracellular matrix, including fibrin, elastin, and collagen, eventually leading to immune evasion and dissemination within the host (Chadha et al. 2021b). The successful production of these virulence determinants is critical for bacterial pathogenesis and establishment of infection (Chadha et al. 2023b). The production of pyocyanin, total protease, hemolysin, and pyochelin was

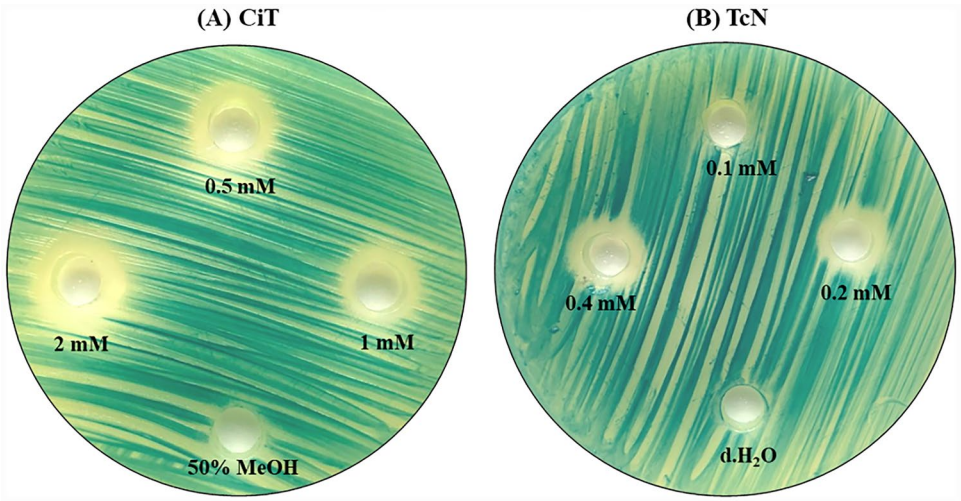

Fig. 2 Qualitative biosensor assay employing *A. tumefaciens* NTL4 to examine the anti-QS potential of CiT (**A**) and TcN (**B**) at various test concentrations (50% MeOH and d.H_2O were used as solvent controls)

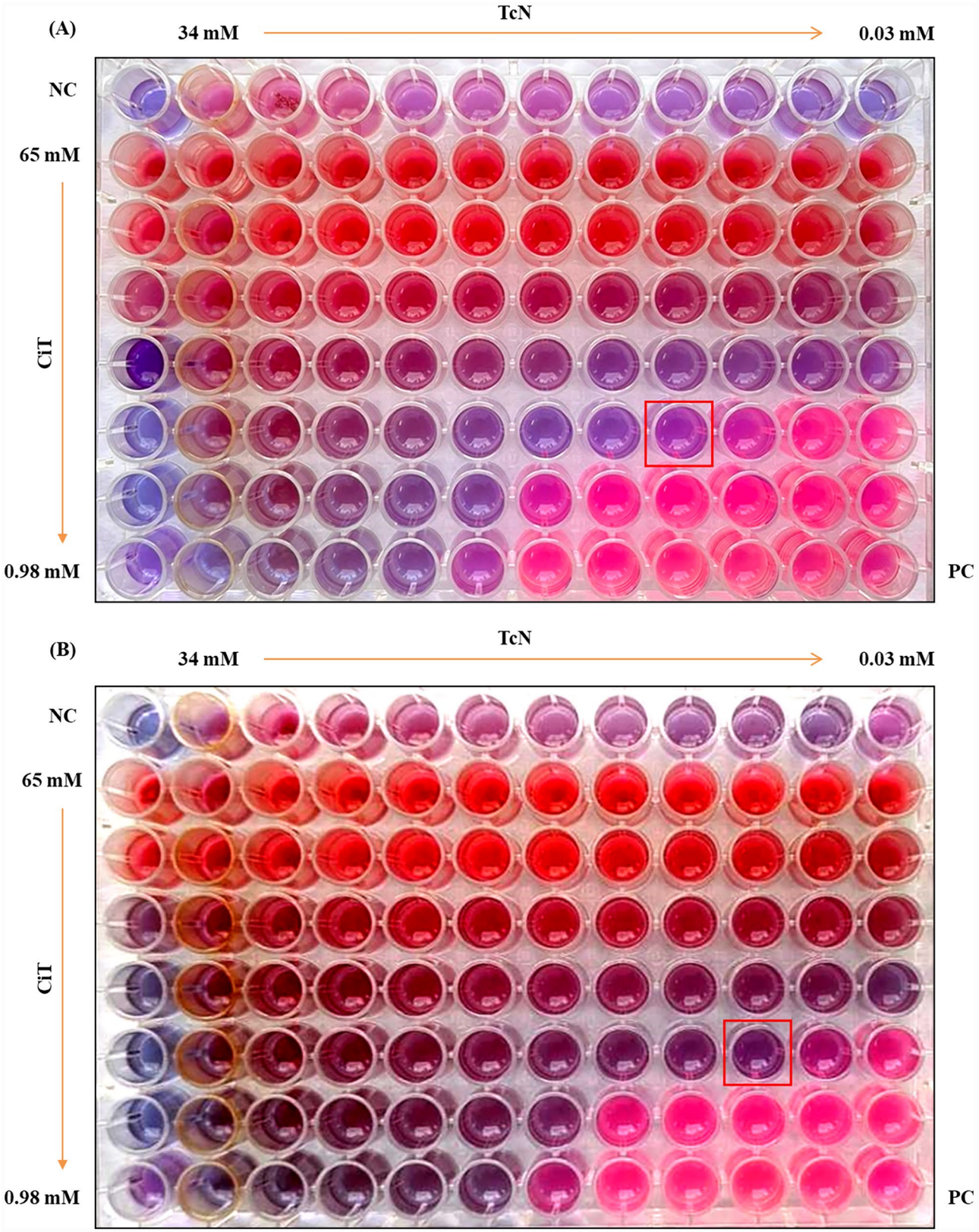

Fig. 3 Checkerboard assay depicting synergistic interaction between CiT and TcN against *P. aeruginosa* **A** PAO1 and **B** PA14. *NC* negative control, *PC* positive control

quantified to be 9.346 ± 1.207 µg/mL, 0.852 ± 0.021 SPAU, 1.116 ± 0.192 mg/mL, and 5.82 ± 0.293 µg/mL in *P. aeruginosa* PAO1, and 12.31 ± 0.955 µg/mL, 0.889 ± 0.023 SPAU, 1.571 ± 0.192 mg/mL, and 7.37 ± 0.595 µg/mL in PA14, respectively (Fig. 4). Interestingly, treatment with CiT-TcN significantly inhibited the production of all virulence factors as compared to the solo-treatment groups (Fig. 4). Solo treatment with TcN was more effective over CiT in curtailing the production of virulence factors in *P. aeruginosa*. In *P. aeruginosa* PAO1, treatment with CiT reduced pyocyanin, total protease, hemolysin, and pyochelin production by 61.5, 12.6, 77.6, and 29.9%; while TcN could effectively lower the same by 83.4, 36.2, 83.9, and 38.4%, respectively. Against *P. aeruginosa* PA14, solo treatments with CiT and TcN were able to achieve reductions up to 64.1, 13.04, 84.2, 14.5% and 63.8, 35.4, 89.5, 32.4%, respectively. In comparison with the untreated control groups, CiT-TcN combination was further able to heighten the antivirulence response in *P. aeruginosa* PAO1 and PA14 by impeding the production of above-mentioned virulence factors by 94.93, 69.7, 94.94, 56.9% and 93.1, 70.1, 97.8, 65.9%, respectively (Fig. 4). Therefore, it is evident that combining CiT and TcN, which are two potent QQ agents exhibiting synergy, can effectively curtail the production of QS-driven virulence factors of *P. aeruginosa*, thereby disarming bacterial virulence at the phenotypic level. Similar findings have been documented in recent literature wherein combinational treatment with QQ drugs (phytochemicals and antibiotics) showing synergy results in heightened antivirulence response against bacterial pathogens including *P. aeruginosa* (Dhara and Tripathi 2019; Johansen et al. 2022; Chadha et al. 2024b). Hence, the combination of CiT and TcN remarkably silences pseudomonal virulence in vitro. Nevertheless, other QS-regulated virulence factors such as exotoxin A, type III secretion system, hydrogen cyanide, and elastases/proteases can also be phenotypically/genotypically tested to assess the antivirulence prospects of the drug combination more holistically.

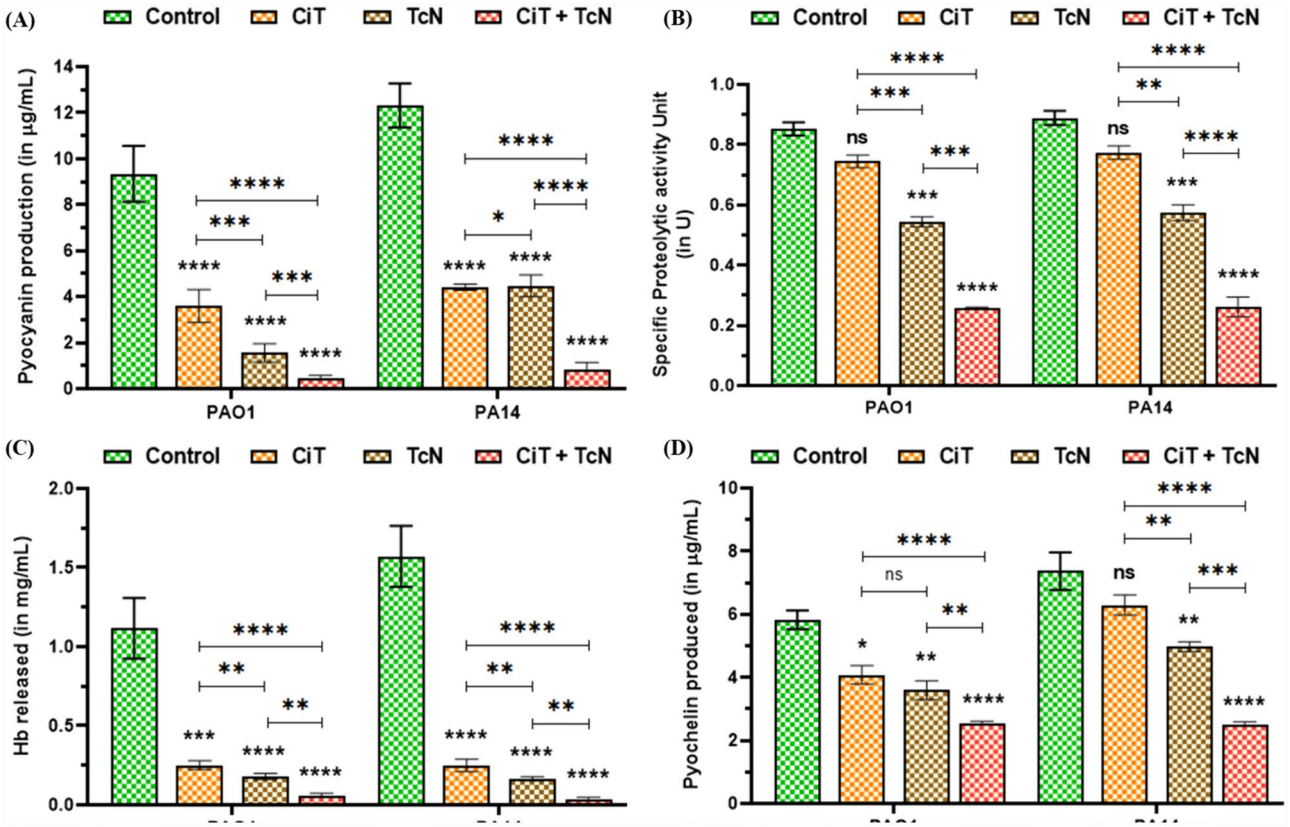

Fig. 4 Quantitative assays for examining the antivirulence potential of CiT (3.92 mM) and TcN (0.12 mM), alone and in combination, against *P. aeruginosa* PAO1 and PA14. Hallmark QS-regulated virulence hallmarks of *P. aeruginosa* were estimated, including **A** pyocyanin, **B** total protease activity, **C** hemolysin, and **D** pyochelin production (significance values over individual bar graphs indicate statistical differences with respect to control, while others indicate statistical differences across experimental groups; *ns* no significance, $*p \leq 0.05$, $**p \leq 0.01$, $***p \leq 0.001$, $p**** \leq 0.0001$)

Combinational treatment with CiT and TcN prevents biofilm formation in *P. aeruginosa*

Biofilm formation is one of the hallmark virulence determinants of *P. aeruginosa* that plays a quintessential role in imparting drug resistance, evasion against immunosurveillance proteins and phagocytic cells, thereby promoting bacterial persistence and resilience (Chadha et al. 2021b). Moreover, it is intricately linked with the QS mechanisms of the pathogen. Hence, we probed whether CiT-TcN combination could avert pseudomonal biofilm formation on glass tubes. To test this hypothesis, a qualitative CV-binding assay was employed and biofilm formation was assessed as a function of CV bound (adhered biofilm cells) to glass surface (Chadha et al. 2022). Interestingly, *P. aeruginosa* PAO1 and PA14 formed strong biofilms (indicated by + ++) on glass tubes which was evident from the intensity of bound CV (Fig. 5). Solo treatment with CiT at sub-MICs was capable of lowering pseudomonal biofilms to a moderate level (++), while TcN notably resulted in the development of a weaker biofilm (+) in both PAO1 (Fig. 5A) and PA14 (Fig. 5B). To our interest, combinational treatment with CiT and TcN resulted in complete loss of bacterial biofilm (denoted by -) since there was no bound CV detected. Moreover, upon eluting the bound CV, it was found that untreated (control) PAO1/PA14 showed notable biofilm formation, while solo and combinational treatment with CiT and TcN resulted in effective biofilm inhibition (Fig. 5C). It was evident that TcN was more efficient over CiT in preventing biofilm formation in *P. aeruginosa*. In PAO1, CiT and TcN individually were capable of inhibiting biofilm formation by 67.2 and 92.5%, respectively. On the other hand, solo treatment extended biofilm inhibition in PA14 by 43.3 and 92.1%, respectively. However, the combination of CiT and TcN showed enhanced anti-biofilm potential by abrogating pseudomonal biofilms of PAO1 and PA14 by 98.52 and 98.74%, respectively (Fig. 5C). Our findings are in accordance with previous literature that highlights the anti-biofilm properties of CiT (Batohi et al. 2021) and TcN (Parsek et al. 2020) against *C. violaceum* and *P. aeruginosa*, respectively, through disruption of membrane potential. Hence, the anti-biofilm potential of this drug combination was confirmed both qualitatively and quantitatively, which may be extended for biomedical application upon subsequent experimentation and validation. Additionally, the existing literature confirms the non-toxic/safety profile of orally- and topically-administered CiT in murine models without inducing any genotoxic effects over long periods (National Toxicology Program 2003; Nordin et al. 2018). Contrarily, TcN extends cytotoxic and genotoxic effects in mammalian cells, including blood mononuclear cells, keratinocytes, porcine spermatozoa, and murine pancreatic cells, even at extremely low drug concentrations of 1–10 µg/mL (Ajao et al. 2015). It also impairs oxidative phosphorylation via uncoupling of ATP synthetase complex V in the mitochondria of rat liver cells. Moreover, TcN (0.1–2 mg/L) has been shown to lower worm reproduction, lifespan, and delayed hatching alongside inducing oxidative stress in *Caenorhabditis elegans* within 24 h of exposure (Lenz et al. 2017). In view of the above-mentioned studies, it can be inferred that CiT-TcN combination should be not considered for oral/systemic administration, but rather be exploited for topical application involving disinfection/

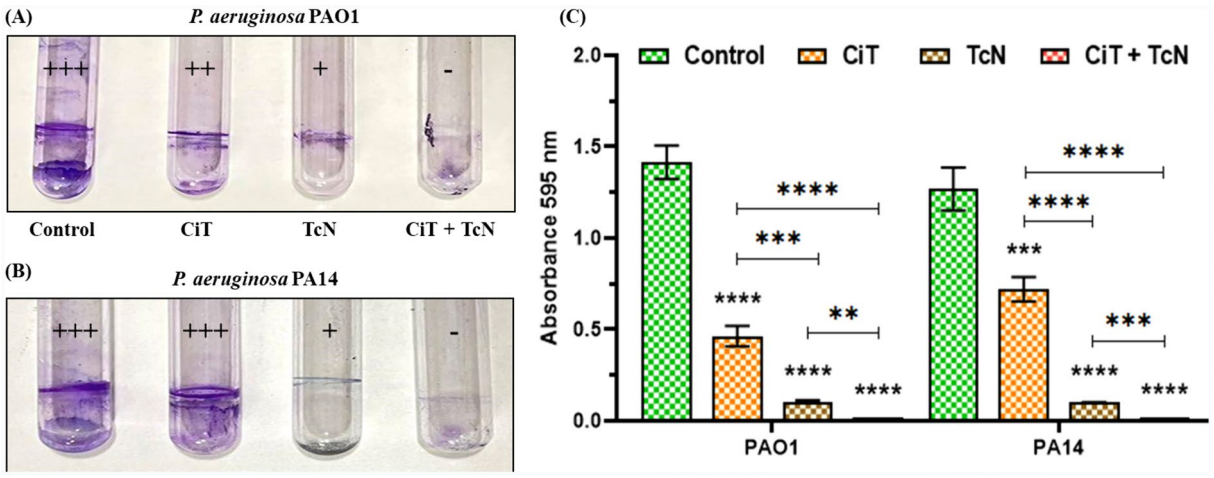

Fig. 5 CV-binding assay for assessing biofilm inhibition effect of CiT (3.92 mM) and TcN (0.12 mM), alone and in combination, against *P. aeruginosa* PAO1 and PA14. (A, B) Qualitative assay. Adherence scores have been depicted on top of the tubes (+++): strong adherence, (++): moderate adherence, (+): weak adherence, (−): no adherence. (C) Quantitative assay depicting A_{595} values corresponding to biofilm inhibition in terms of CV adherence to glass tubes (significance values over individual bar graphs indicate statistical differences with respect to control, while others indicate statistical differences across experimental groups; $^{**}p \leq 0.01$, $^{***}p \leq 0.001$, $p^{****} \leq 0.0001$)

sanitization of surfaces, fomites, and even biomedical devices such as urinary catheters.

Computational studies predict strong molecular interactions between QS receptor and test drugs

AutoDock Vina is an excellent tool that provides computational insights by predicting the probable molecular interactions between test ligand(s) and a receptor (Gulati et al. 2023). With respect to QQ, ligands that demonstrate high-binding affinity towards QS receptors have been shown to interfere with bacterial signaling pathways, consequently disarming pseudomonal virulence through inhibition (competitive) of QS signal transduction (Chadha et al. 2024a). Since CiT and TcN exhibited remarkable anti-QS and anti-virulence prospects, we further tested their ability to associate with the QS receptors of *P. aeruginosa* using molecular docking. The natural ligands (3-oxo-C12-HSL, C4-HSL, and PQS) were used as control molecules for the respective QS receptor alongside a known QS inhibitor, furanone C-30. As anticipated, both the drugs formed strong molecular interactions with the LasR, PqsR, and RhlR receptors (Fig. 6). The binding energies for all control and test ligands towards the QS receptors have been collated along with their interacting amino acid residues in Table 1. Interestingly, CiT and TcN formed multiple hydrogen bonds (H-bonds), van der Waal (vdW) interactions (hydrophobic bonds), π-cation bonds (electrostatic interactions), and non-covalent bonds (π-alkyl and π-sigma) with all three QS receptors (Fig. 6). Interestingly, the binding energies obtained with TcN revealed stronger molecular associations with all the QS receptors as compared to CiT as well as the control ligands (Table 1). This positively correlates with the previous findings of the study where solo treatment with TcN at sub-inhibitory levels extended greater antivirulence effect over CiT (alone) against *P. aeruginosa*, that too at lower drug concentrations. Furthermore, the binding energies obtained with CiT and TcN were comparable to that of a QQ monoterpene, α-terpineol (between − 5.8 and − 7.1 kcal/mol) (Chadha et al. 2023b). Contrarily, the test drugs exhibited lower binding energies than cinnamaldehyde (between − 7.6 and − 12.0 kcal/mol), a strong QQ phytochemical with profuse antivirulence potential against *P. aeruginosa* (Chadha et al. 2022). These results are in agreement with recent studies that establish a direct

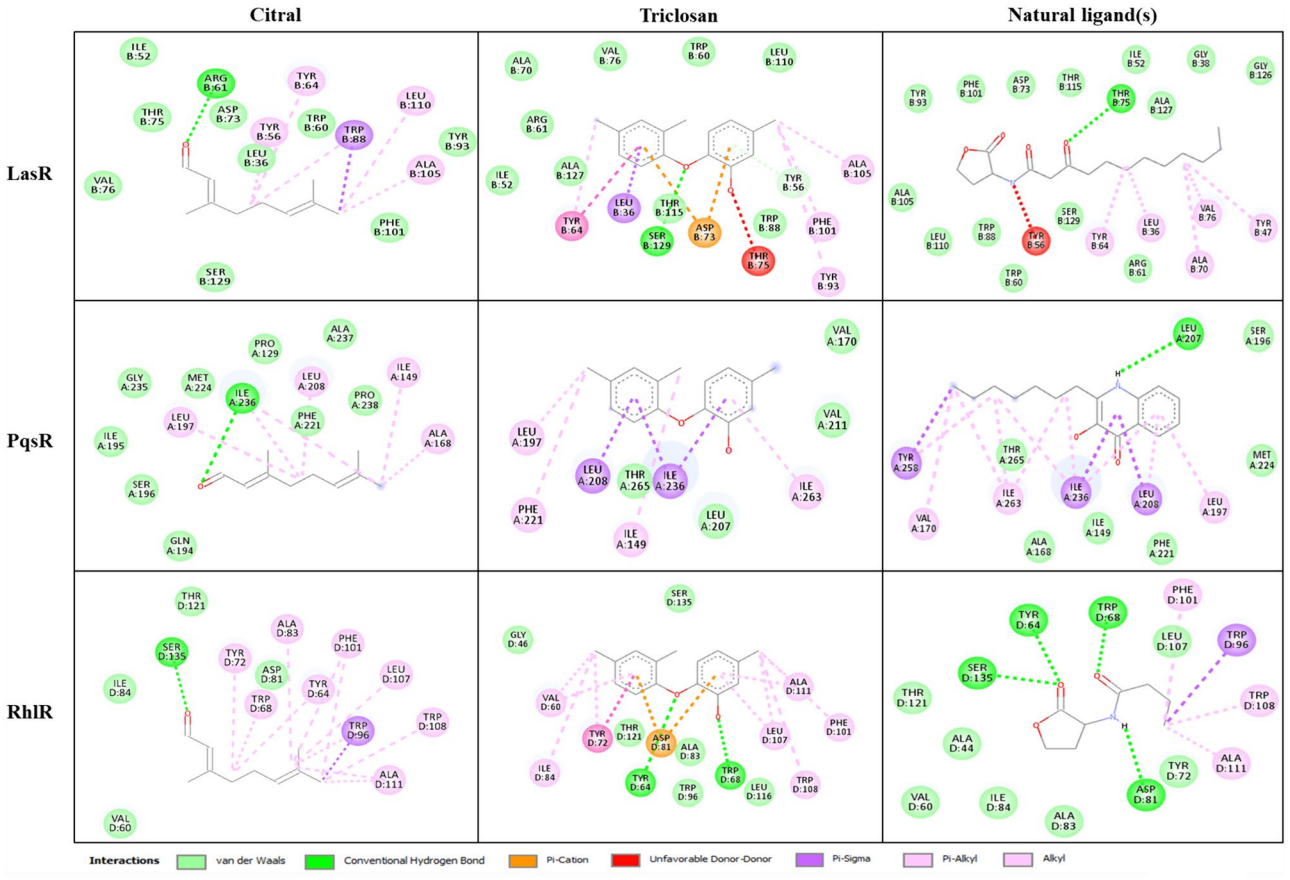

Fig. 6 Two-dimensional representation of molecular interactions predicted between CiT/TcN/natural ligands and various QS receptors of *P. aeruginosa* (LasR, PqsR, and RhlR) using AutoDock Vina (Version 1.5.4)

correlation between the QQ/antivirulence prospects of phytochemicals/antibiotics/FDA-approved drugs and their ability to form high-affinity molecular interactions with the QS receptors of *P. aeruginosa* (Kumar et al. 2021; Chadha et al. 2024a). Therefore, based on the experimental findings, it can be speculated that CiT and TcN strongly associate with the ligand-binding domains of the QS receptors, consequently disrupting QS signal reception and ultimately potentiating an antivirulence response in *P. aeruginosa*. Hence, this study is the first to provide the experimental basis supporting the antivirulence prospects of CiT-TcN combination for disarming pseudomonal virulence in vitro.

Conclusion

In view of the current experimentation, this study provides the first insight into the synergistic interactions between CiT and TcN against *P. aeruginosa*. The findings indicate that treatment with CiT-TcN combination at sub-lethal level potentiates remarkable QQ, which thereby promotes a heightened antivirulence response in *P. aeruginosa*. As a consequence, QS mechanisms are silenced and bacterial virulence is attenuated. Experimental findings (in vitro) supporting the anti-QS and antivirulence potential were further validated from molecular docking studies (in silico analysis) that predicted high-affinity interactions between the QS receptors and CiT/TcN, probably responsible for disrupting QS signal transduction. Nevertheless, pre-clinical studies are further warranted to assess the antivirulence potential of CiT-TcN combination against drug-resistant clinical strains of *P. aeruginosa*. This would provide more insights and lay substantial grounds for this drug combination to be explored in vivo. Thus, as a viable and potent alternative to existing antimicrobial treatments, bioactive compounds with notable antivirulence properties can serve as emerging strategy to combat pseudomonal infections.

Supplementary Information The online version contains supplementary material available at https://doi.org/10.1007/s00203-024-04059-4.

Acknowledgements The authors would like to acknowledge the Department of Microbiology, Panjab University, Chandigarh, for providing the infrastructure to execute this study. Financial assistance from the Indian Council of Medical Research (ICMR), Govt. of India, New Delhi, to JC and LK is also appreciated.

Author contributions JC: Idea conceptualization, experimental design and initiation, methodology, data analysis and curation, and manuscript writing, review, and editing. PA: Experimental design and initiation, execution (in vitro), methodology, data analysis and curation, and manuscript writing. UM: Execution (in silico), methodology, data analysis and curation, LK: Formal analysis, manuscript writing and editing. KH: supervision, continuous motivation, resources, data analysis, critical analysis, and manuscript editing. All authors read and approved the final version of this manuscript.

Funding The authors did not receive any specific grant from funding agencies in the public, commercial, or not-for-profit sectors.

Data availability Data used to support the findings of this study are available from the corresponding author upon request.

Declarations

Conflict of interest We declare that we have no conflicts of interest to declare.

Consent for publication This manuscript is original and not published elsewhere. All authors have read and approved the final manuscript, and confirm that there are no ethical issues associated with the publication of this manuscript.

References

Ajao C et al (2015) Mitochondrial toxicity of triclosan on mammalian cells. Toxicol Rep 2:624–637. https://doi.org/10.1016/j.toxrep.2015.03.012

Batohi N, Lone SA, Marimani M, Wani MY, Al-Bogami AS, Ahmad A (2021) Citral and its derivatives inhibit quorum sensing and biofilm formation in Chromobacterium violaceum. Arch Microbiol 203:1451–1459. https://doi.org/10.1007/s00203-020-02127-z

Bose SK, Chauhan M, Dhingra N, Chhibber S, Harjai K (2020) Terpinen-4-ol attenuates quorum sensing regulated virulence factors and biofilm formation in Pseudomonas aeruginosa. Future Microbiol 15:127–142. https://doi.org/10.2217/fmb-2019-0204

Cao Y, Zhou D, Zhang X, Xiao X, Yu Y, Li X (2021) Synergistic effect of citral and carvacrol and their combination with mild heat against Cronobacter sakazakii CICC 21544 in reconstituted infant formula. Lwt 138:110617. https://doi.org/10.1016/j.lwt.2020.110617

Chadha J (2021) In vitro effects of sub-inhibitory concentrations of amoxicillin on physiological responses and virulence determinants in a commensal strain of Escherichia coli. J Appl Microbiol 131:682–694. https://doi.org/10.1111/jam.14987

Chadha J, Khullar L (2021) Subinhibitory concentrations of nalidixic acid alter bacterial physiology and induce anthropogenic resistance in a commensal strain of Escherichia coli in vitro. Lett Appl Microbiol 73:623–633. https://doi.org/10.1111/lam.13550

Chadha J et al (2021a) Antibacterial potential of indigenous plant extracts against multidrug-resistant bacterial strains isolated from New Delhi region. GSC Biol Pharm Sci 14:185–196. https://doi.org/10.30574/gscbps.2021.14.2.0053

Chadha J, Harjai K, Chhibber S (2021b) Repurposing phytochemicals as anti-virulent agents to attenuate quorum sensing-regulated virulence factors and biofilm formation in Pseudomonas aeruginosa. Microb Biotechnol 15:1695–1718. https://doi.org/10.1111/1751-7915.13981

Chadha J, Harjai K, Chhibber S (2021c) Revisiting the virulence hallmarks of Pseudomonas aeruginosa: a chronicle through the perspective of quorum sensing. Environ Microbiol 24:2630–2656. https://doi.org/10.1111/1462-2920.15784

Chadha J, Ravi SJ, Chhibber S, Harjai K (2022) Gentamicin augments the quorum quenching potential of cinnamaldehyde in vitro and protects caenorhabditis elegans from pseudomonas aeruginosa infection. Front Cell Infect Microbiol. https://doi.org/10.3389/fcimb.2022.899566

Chadha J, Khullar L, Gulati P, Chhibber S, Harjai K (2023a) Antivirulence prospects of metformin against pseudomonas aeruginosa: a new dimension to a multifaceted drug. Microb Pathog 183:106281. https://doi.org/10.1016/j.micpath.2023.106281

Chadha J, Ravi SJ, Harjai K (2023b) α-Terpineol synergizes with gentamicin to rescue Caenorhabditis elegans from Pseudomonas aeruginosa infection by attenuating quorum sensing-regulated virulence. Life Sci 313:121267. https://doi.org/10.1016/j.lfs.2022.121267

Chadha J, Khullar L, Gulati P, Chhibber S, Harjai K (2024a) Repurposing albendazole as a potent inhibitor of quorum sensing-regulated virulence factors in pseudomonas aeruginosa: novel prospects of a classical drug. Microb Pathog 186:106468. https://doi.org/10.1016/j.micpath.2023.106468

Chadha J, Moudgil G, Harjai K (2024b) Synergism between α-terpineol and terpinen-4-ol potentiates antivirulence response against pseudomonas aeruginosa. Ind J Microbiol. https://doi.org/10.1007/s12088-024-01189-7

Dai J, Bai M, Li C, San Cheang W, Cui H, Lin L (2023) Antibacterial properties of citral against Staphylococcus aureus: from membrane damage to metabolic inhibition. Food Biosci 53:102770. https://doi.org/10.1016/j.fbio.2023.102770

Dhara L, Tripathi A (2019) Cinnamaldehyde: a compound with antimicrobial and synergistic activity against ESBL-producing quinolone-resistant pathogenic Enterobacteriaceae. Eur J Clin Microbiol 39:65–73. https://doi.org/10.1007/s10096-019-03692-y

Fidaleo M, Zuorro A, Lavecchia R (2013) Enhanced antibacterial and anti-quorum sensing activities of triclosan by complexation with modified β-cyclodextrins. World J Microbiol Biotechnol 29:1731–1736. https://doi.org/10.1007/s11274-013-1335-z

Gulati P, Chadha J, Harjai K, Singh S (2023) Targeting envelope proteins of poxviruses to repurpose phytochemicals against monkeypox: An in silico investigation. Front Microbiol. https://doi.org/10.3389/fmicb.2022.1073419

Harjai K, Gupta P, Chhibber S (2016) Subinhibitory concentration of ciprofloxacin targets quorum sensing system of Pseudomonas aeruginosa causing inhibition of biofilm formation & reduction of virulence. Ind J Med Res 143:643. https://doi.org/10.4103/0971-5916.187114

Johansen B, Duval R, Sergere J-C (2022) First evidence of a combination of terpinen-4-ol and α-terpineol as a promising tool against ESKAPE pathogens. Molecules 27:7472. https://doi.org/10.3390/molecules27217472

Kang S et al (2022) Antibacterial effect of citral on yersinia enterocolitica and its mechanism. Food Control 135:108775. https://doi.org/10.1016/j.foodcont.2021.108775

Kaur A, Gautam LK, Balda S, Capalash N, Sharma P (2022) Triclosan controls pleiotropically the paper-deteriorating bacterial community in paper mill. Int Biodeter Biodegr 173:105455. https://doi.org/10.1016/j.ibiod.2022.105455

Kumar L, Brenner N, Brice J, Klein-Seetharaman J, Sarkar SK (2021) Cephalosporins interfere with quorum sensing and improve the ability of caenorhabditis elegans to survive pseudomonas aeruginosa infection. Front Microbiol. https://doi.org/10.3389/fmicb.2021.598498

Laxminarayan R (2022) The overlooked pandemic of antimicrobial resistance. Lancet 399:606–607. https://doi.org/10.1016/s0140-6736(22)00087-3

Lenz KA, Pattison C, Ma H (2017) Triclosan (TCS) and triclocarban (TCC) induce systemic toxic effects in a model organism the nematode Caenorhabditis elegans. Environ Pollut 231:462–470. https://doi.org/10.1016/j.envpol.2017.08.036

Manganelli R et al (2016) Antimicrobial activity and possible mechanism of action of citral against cronobacter sakazakii. PLoS ONE 11:e0159006. https://doi.org/10.1371/journal.pone.0159006

Moradali MF, Ghods S, Rehm BHA (2017) Pseudomonas aeruginosa lifestyle: a paradigm for adaptation, survival, and persistence. Front Cell Infect Microbiol. https://doi.org/10.3389/fcimb.2017.00039

National Toxicology Program (2003) NTP toxicology and carcinogeneisss studies of citral (microencapsulated) (CAS No. 5392–40-5) in F344/N rats and B6C3F1 mice (feed studies). Natl Toxicol Program Tech Rep Ser 505:1–268

Nordin N et al (2018) Characterization and toxicity of citral incorporated with nanostructured lipid carrier. PeerJ 6:e3916. https://doi.org/10.7717/peerj.3916

Parsek M, Maiden MM, Waters CM (2020) Triclosan depletes the membrane potential in Pseudomonas aeruginosa biofilms inhibiting aminoglycoside induced adaptive resistance. PLoS Pathog 16:e1008529. https://doi.org/10.1371/journal.ppat.1008529

Qin S et al (2022) Pseudomonas aeruginosa: pathogenesis, virulence factors, antibiotic resistance, interaction with host, technology advances and emerging therapeutics. Signal Transduct Target Ther. https://doi.org/10.1038/s41392-022-01056-1

Sharma A, Harjai K, Ramniwas S, Singh D, Yi DK (2023) Bioactivity of citral and its nanoparticle in attenuating pathogenicity of pseudomonas aeruginosa and controlling drosophila melanogaster. J Nanomater 2023:1–11. https://doi.org/10.1155/2023/4703650

Shrestha P, Ni J, Wong T-Y (2020) Synergistic and antagonistic interactions of triclosan with various antibiotics in bacteria. J Environ Sci Health C 38:187–203. https://doi.org/10.1080/26896583.2020.1781494

Sinicropi MS et al (2022) Triclosan: a small molecule with controversial roles. Antibiotics 11:735. https://doi.org/10.3390/antibiotics11060735

Tabak M, Scher K, Chikindas ML, Yaron S (2009) The synergistic activity of triclosan and ciprofloxacin on biofilms of Salmonellaâ€ƒTyphimurium. FEMS Microbiol Lett 301:69–76. https://doi.org/10.1111/j.1574-6968.2009.01804.x

Valliammai A, Selvaraj A, Mathumitha P, Aravindraja C, Pandian SK (2021) Polymeric antibiofilm coating comprising synergistic combination of citral and thymol prevents methicillin-resistant Staphylococcus aureus biofilm formation on titanium. Mater Sci Eng C 121:111863. https://doi.org/10.1016/j.msec.2021.111863

Wiegand I, Hilpert K, Hancock REW (2008) Agar and broth dilution methods to determine the minimal inhibitory concentration (MIC) of antimicrobial substances. Nat Protoc 3:163–175. https://doi.org/10.1038/nprot.2007.521

World health Organisation (2024) WHO updates list of drug-resistant bacteria most threatening to human health. https://www.who.int/news/item/17-05-2024-who-updates-list-of-drug-resistant-bacteria-most-threatening-to-human-health. Accessed on 5 June 2024